Evaluation of surface roughness and wall thickness in the incremental stamping process with variation in the degrees of freedom of the contact tool

Gilmar Cordeiro Silva (gilmarcord@gmail.com)
Pontificia Universidade Catolica de Minas Gerais https://orcid.org/0000-0002-5405-8086
Lucas Moraes Rufini Souza
Pontificia Universidade Catolica de Minas Gerais
Lucio Flavio Santos Patrício
Centro Federal de Educação Tecnológica

Research Article

Keywords: incremental stamping, aluminium alloy, rotational tool, single point incremental forming, roughness, thickness distribution

Posted Date: May 14th, 2021

DOI: https://doi.org/10.21203/rs.3.rs-506695/v1

Evaluation of surface roughness and wall thickness in the incremental stamping process with variation in the degrees of freedom of the contact tool

Gilmar Cordeiro da Silva[1], Lucas Moraes Rufini de Souza[2], Lucio Flávio Santos Patrício[3]

1. Gilmar Cordeiro da Silva: Mechanical Engineering Department, Pontifícia Universidade Católica de Minas Gerais – PUC Minas, Belo Horizonte, MG, Brazil. Avenida Dom José Gaspar, 500 – Campus Coração Eucarístico – CEP. 30545-901 – Graduate program in mechanical engineering – Tel. +55 31 33194910. E-mail: *gilmarcord@gmail.com.* (Corresponding author).

2. Lucas Moraes Rufini de Souza: Mechanical Engineering Department, Pontifícia Universidade Católica de Minas Gerais – PUC Minas, Belo Horizonte, MG, Brazil. Avenida Dom José Gaspar, 500 – Campus Coração Eucarístico – CEP. 30545-901. Tel. +55 32 988041725. E-mail: *rufinilucas@gmail.com*.

3. Lucio Flávio Santos Patrício: Mechanical Engineering Department, Centro Federal de Educação Tecnológica, Rua Álvares de Azevedo, 400 - Bela Vista, Divinópolis - MG, CEP 35503-822, Brazil– Tel. +55 37 999073407. E-mail: *lucio@cefetmg.br*.

*** Corresponding author:** Gilmar Cordeiro da Silva, Department of Mechanical Engineering, Pontifícia Universidade Católica de Minas Gerais – PUC Minas, Belo Horizonte, Brazil, MG, Av. Dom José Gaspar 500 – Coração Eucarístico. Tel.: +55-31-3319-4910, E-mail: gilmarcord@gmail.com

ABSTRACT

In this study, the performance of a rotating semi-spherical tool (with two degrees of freedom) is compared with another rigid semi-spherical tool, both with a diameter of 8.0 mm. The stamping is performed on AA1100 aluminium blanks with a thickness of 0.8 mm, using a helical strategy and single point incremental forming technique, with a feed rate of 1000 mm/min, a step depth of 0.1 mm, without rotation on the machine spindle and petroleum jelly as a lubricant. The behaviour of R_a and R_q roughness and wall thickness is evaluated during the tests. Scanning electron microscopy and dispersive energy spectroscopy are used to observe the wear mechanisms on the surface of the samples. On this basis, the tools for incremental stamping must promote continuous contact with the blank without generating excessive

friction. Our results show that the rigid tool presents the best working conditions for the AA1100 aluminium sheets because it generates less roughness in the stamped parts, when compared with the rotating tool (~54% lower in the final average of the R_a roughness). The scanning electron microscopy image reveals the presence of adhesion both on the contact tip of the rotational tool and on the rigid tool, showing that the adhesive wear mechanism is predominant in the single point incremental forming process and influences the final roughness of the stamping cones.

Keywords: incremental stamping, aluminium alloy, rotational tool, single point incremental forming, roughness, thickness distribution

1 INTRODUCTION

The incremental sheet forming (ISF) process has emerged as a promising method for forming sheets in small batches. This process is efficient and provides cost reductions in the manufacturing process, making it a potential alternative to the conventional sheet stamping process [[1]–0].

Incremental stamping allows for the advanced manufacturing of parts, using only a tool with a determined geometry, a plate, a blank holder, a lubricant and a computer numerical control machine [0, 0]. Four parameters are relevant to this process, namely, the feed rate, tool diameter, vertical increment and sheet thickness [0, 0, 0]. Two techniques for incremental stamping are utilised according to the number of contact points, namely, single point incremental forming (SPIF) and two point incremental forming (TPIF) [[8], 0]. In the SPIF process, the plate is supported on the blank holder and the deformation is applied by the tool that moves on the surface. In the TPIF, the plate is pressed by the blank holder and simultaneously by two tools, which provides greater alternatives to the process, and can be used with a partial or total matrix instead of a second tool [0, 0-0]. This technology has been mainly used in the automotive and aeronautical sectors, with aluminium alloys representing some of the most researched materials [0, 0].

Recently, researchers have turned their attention to understanding the tribological condition as a determining factor for the success of the conformation process. Friction is a variable present in any forming process, especially in incremental stamping [0]. In a study by Sornsuwit and Sittisakuljaroen [0], the surface roughness was influenced by the process parameters, such as the forming depth, the maximum angle of the wall and the thickness of the metal plate, in the SPIF method. Hussain and Gao [0] studied a method to test

the conformation limit of a material (maximum angle of the wall) based on the law of sines, according to Eq. (1):

$$t_d = \frac{t_0 y_d}{R} \tag{1}$$

where t_0 is the initial plate thickness, y_d is the fracture depth, R is the radius of the generatrix and t_d is the thickness in the fracture region, as shown in **Error! Reference source not found.**.

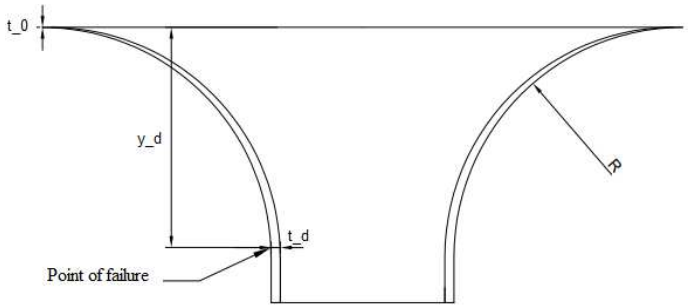

Fig. 1. CAD model of a truncated cone [adapted from 0, 0]

Azhiri *et al*. [0] studied the effect of tool geometry on the performance of the incremental stamping of 5052 aluminium with a thickness of 1.5 mm and blank dimensions of 25 mm by 25 mm. Two tools were used, one with a ball nose tool and the other with a rigid tip, and both contact points were manufactured with AISI H13 steel. Their results revealed that the use of a ball nose tool improved the formability and the quality of the surface. In addition, it was found that the best results for the surface roughness were obtained with the ball nose tool, with a feed rate of 200 mm/min and a vertical increase of 0.2mm, without using the rotation speed of the machine.

De Castro Maciel *et al*. [0] investigated the relation between the limit angle of the wall and the thickness of AA1100 aluminium alloys and magnesium AZ31-B alloy in the SPIF method. In the tests, a rotating spherical tool was used with 1.0 mm-thick plates, a feed rate of 1500 mm/min, a vertical increment of 0.01 mm and no rotation speed (0 rpm). The results obtained show that there was adhesion on the tip of the tool used in the AZ31-B alloy and this fact influenced the fracture of the material and can be used as an indicator of premature fracture of the material.

Despite several previous studies being related to incremental stamping, the analysis of the influence of the degrees of freedom of the contact tool on the surface roughness and wall thickness has not yet been evaluated for AA1100 aluminium sheets. The purpose of this work is to employ two tools (rigid and rotating) with different degrees of freedom in the ISF process to investigate their influence on the variation of the roughness and thickness of AA1100 aluminium sheets. Additionally, the adhesion at the tip of the tools is analysed to verify its influence on the finishing of the parts.

2 MATERIALS AND METHODS

The sheet material used in the incremental stamping was characterised via optical emission spectroscopy as an AA1100 aluminium alloy. The chemical composition of the main elements of this alloy can be seen in Table 1.

Table 1. Chemical composition of AA1100 alloy

Elemental composition (%)						
Al	Si	Fe	Mn	Mg	Li	Others
99.5902	0.0395	0.2382	0.0018	0.0012	0.0001	0.1223

The mechanical properties of aluminium were obtained from a stress test using an Instron 4467 tester with a maximum stress and compression capacity of 30 KN, according to the ASTM E8 standard. For the test, three specimens were manufactured at 0º of the lamination direction. In **Error! Reference source not found.**, the engineering stress-strain curve (average values) for the AA1100 alloy is shown. The obtained curve is similar to that found in [0, 0] with close values for the annealed 1100 series of aluminium sheets. When comparing the results with other authors [0, 0], it is observed that the yield limit is close to the presented resistance limit.

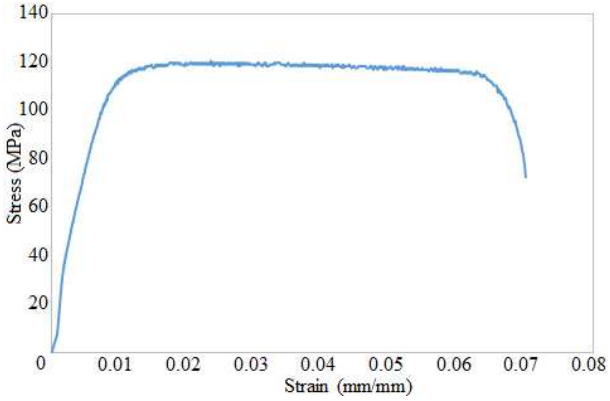

Fig. 2. Behaviour of stress (MPa) versus strain (mm/mm)

For the tests of the SPIF process, rigid and rotating tools (with two degrees of freedom) were used in the 0.8 mm-thick aluminium sheets. The tools (rotating and rigid) were built using the AISI 4140 material by the conventional machining process, both with an 8.0 mm diameter working region. Posteriorly, the thermal treatment of beneficiation was carried out (tempering followed by quenched in both tools). In the tempering, the austenitisation temperature was 855 °C and the material was cooled in oil. To relieve tension, the material was subjected to quenching for 2 h at 200 °C. **Error! Reference source not found.** shows both tools.

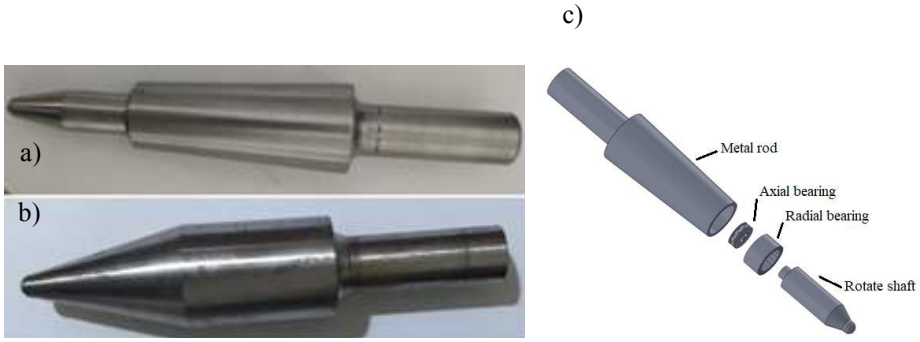

Fig. 3. Tools used in incremental stamping. **(a)** Rigid tool. **(b)** Rotating tool with two degrees of freedom. **(c**) Expanded view of the rotating tool with two degrees of freedom

From the compound movement of the contact between the tool and plate, the rotating tool has two degrees of freedom. One degree of freedom is due to the circular translation movement. In addition to this, it can act, nominally, with a second degree of freedom around its own axis ("z" axis), because as the tool is free in the spindle and has two bearings, the rotation movement of the rotate shaft does not influence in the rotation movement of the metal rod, if it occurs.

Incremental stamping was performed with a computer numerical control machining centre (Travis model M-800). The process parameters are shown in Table 2. Solid petroleum jelly was used as a lubricant due to its better performance [0] compared to other lubricants.

Table 2. Process parameters

Process parameters in tests					
Tool diameter (mm)	Feed rate (mm/min)	Spindle speed	Step depth (mm)	Tool path	Lubricant
8	1000	Free	0.1	Helical	Petroleum jelly

To obtain the maximum angle of the wall, tests were carried out in the SPIF process with a single pass in a truncated cone in the AA1100 alloy (**Error! Reference source not found.**). In addition to the tests on the truncated cone, three straight cones were stamped with each tool for analysis of the roughness and thickness. The single-factor analysis of variance (ANOVA) was used to test the hypothesis.

The surface roughness was evaluated on the inside of the cones, using the roughness parameters (R_a and R_q), with an electronic rugosimeter (Ametek Taylor Hobson model Surtronic S-100). The measurements were collected in the quadrants of the cone, i.e., at 0º, 90º, 180º and 270º. In each quadrant, five equidistant points were measured in the direction of the cone height (**Error! Reference source not found.** shows the sectional view of three of the quadrants). The thickness of the wall, along the length of the straight cone, was measured with a three-dimensional machine of the brand Mitutoyo model QM-messure 353. The thickness measurement points were the same as for the roughness measurement (**Error! Reference source not found.**).

Scanning electron microscopy (SEM) together with energy dispersion X-ray spectroscopy (EDS) was carried out to investigate the surface morphology and its chemical composition using a JEOL model JSM-IT300 with IT 300 software and an OXFORD/X-MaxN detector with Aztec software.

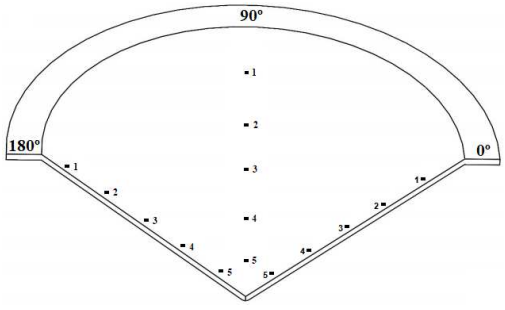

Fig. 4. Measuring points.

3 RESULTS AND DISCUSSION

3.1 Limit angle determination

Error! Reference source not found.(a) shows the internal and external surfaces of the stamped cone with the rotating tool with two degrees of freedom. **Error! Reference source not found.**(b) shows the internal and external surface of the stamped cone with the rigid tool.

Fig. 5. (a) Two degrees of freedom for rotating tool truncated cone and (b) rigid tool truncated cone

Table 3 shows the average values found for the limit angle of the wall of the two tools, according to the depth at which the fracture in the truncated cones occurred. The maximum angle of the wall was obtained from the angle formed between the straight line of the depth at which the fracture occurred and a symmetrical line (tangent) to the fracture that was drawn in the 3D CAD model with the geometry identical to the part (**Error! Reference source not found.**).

Table 3. Maximum wall angle

Maximum angle (º)	
Rotating tool with two degrees of freedom	Rigid tool
77.92° ± 0.38	74.14° ± 0.76

The tests made it possible to verify that the rotating tool with two degrees of freedom showed a greater limit angle for the experiment with the truncated cone geometry. The values of the maximum wall angle were slightly higher than those found by [0] for the 1.0 mm-thick AA1100 aluminium plate using 12 mm diameter tools, a 0.1 mm vertical increment, a 1500 mm/min feed rate, an incremental strategy and petroleum jelly as a lubricant. The diameter of the tool tip is a fundamental parameter of the process because it is directly related to the acting pressure and the geometry obtained. When the diameter of the tool increases, the process becomes more similar to conventional stamping, thus reducing the limits of formability [0, 0]. The conditions of this work with a plate with a smaller thickness (0.8 mm) and a rotating tool with a smaller diameter (8.0 mm) compared to [0] produced a greater maximum wall angle, which was expected according to [0, 0]. In addition to the tool diameter, it is believed that the changes in the stamping strategy and the feed rate promoted the best results for the test of the cone truncated when applied to plates with thicknesses below 1 mm.

3.2 Experiments with straight cone geometry

After determining the maximum angle of the wall with the truncated cone test, an attempt was made to stamp a straight cone with the largest possible wall angle. The tests started with the largest angle of the wall found in the truncated cone test, with less than a 3º margin. Figure 6 shows the results of the stamped cones. The tests were interrupted when the fracture occurred (indicated by the red arrows in).

Fig. 6. Straight cones with fixed wall angle of (a) 75º, (b) 70º and (c) 65º

Under the conditions proposed for the tests, it was not possible to stamp the straight cone with the maximum angle of the wall found in the truncated cone test, as shown in Fig. 6. According to [0], a straight cone with a fixed inclination has a lower deformation limit in relation to the truncated cone, as the instantaneous inclination varies according to its depth (Fig. 7).

"F" is the forming force and "N" is the instantaneous position of the tool during the process. As shown in Fig. 7(a), the resulting force “FSinθ” acts only on the LN segment, which represents a small part of the MN segment. In contrast, in Fig. 7(b), the entire MN segment is under the action of the “FSinθ” force, which weakens the segment, contributing to the fracture of the piece [0].

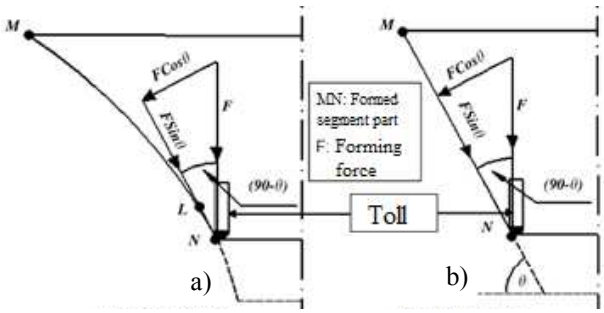

Fig. 7. Comparison of forming forces according to cone geometry: (a) truncated cone; (b) straight cone [adapted from 0]

Thus, the 60º wall angle was used for experiments with the straight cone, because it was the largest possible angle to stamp the 0.8 mm-thick plates with the two types of tools proposed.

Figure 8 shows the internal surface of the cones stamped with both tools on 0.8 mm-thick AA1100 aluminium plates. In the parts stamped with the rotating tool with two degrees of freedom (Fig. 8(a)), a matte appearance is observed. Unlike the stamped part with a rigid tool (Fig. 8(b)), where a mirrored surface was observed. The average roughness values (R_a and R_q) obtained in the tests for both tools can be seen in Table 4.

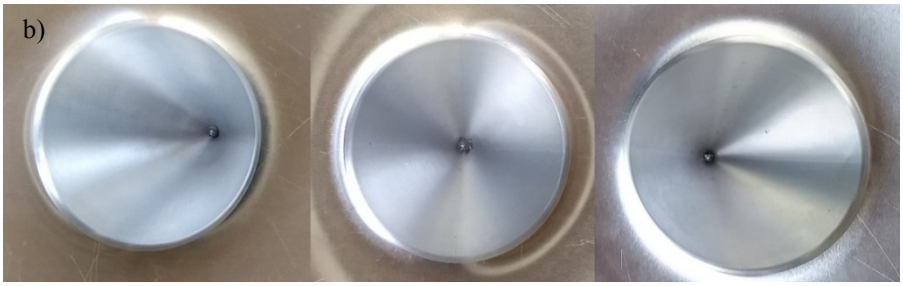

Fig. 8. (a) Stamped parts with two degrees of freedom rotating tool. (b) Stamped parts with rigid tool

3.3 Roughness and thickness of the parts

Table 4 shows the average of the results measured for the R_a and R_q roughness on the inner surface of the cones. Figure 9 presents the average of the measured roughness.

Table 4. Measured roughness

Final medium roughness				
	Ra (µm)		Rq (µm)	
	Rotating tool of two degrees of freedom	Rigid tool	Rotating tool of two degrees of freedom	Rigid tool
Region 0º	0.84 ± 0.09	0.49 ± 0.08	1.27 ± 0.27	0.71 ± 0.1
Region 90º	0.88 ± 0.13	0.49 ± 0.07	1.33 ± 0.23	0.71 ± 0.07
Region 180º	0.86 ± 0.09	0.5 ± 0.10	1.3 ± 0.26	0.76 ± 0.25
Region 270º	0.81 ± 0.12	0.49 ± 0.05	1.25 ± 0.28	0.72 ± 0.1

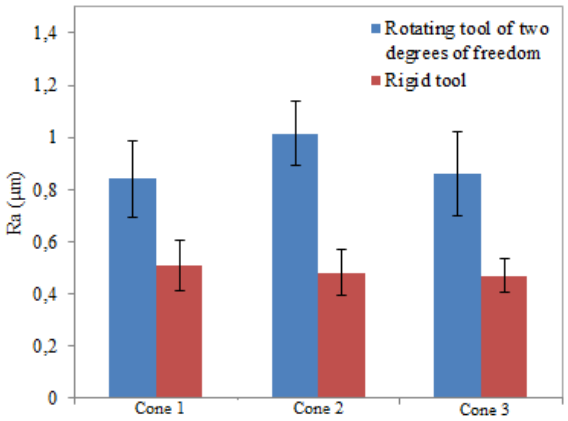

Fig. 9. Roughness R_a (µm)

It was observed that the surface roughness varied with the depth of the straight cone, as reported in [0]. The rigid tool provided lower values of roughness (R_a and R_q) in the stamped parts, when compared to the rotating tool with two degrees of freedom (Fig. 9). Although the tools have the same apparent contact area, due to the identical diameter and the use of the same incremental stamping parameters, it is believed that the working condition imposed on the tool/plate interface was different for each tool. This explains the slight variation in roughness, since, in the tests performed, the rotation on the machine's spindle was zero (zero rpm), which made it possible for both tools to move freely in the spindle (spindle). As the rotary tool with two degrees of freedom has free rotation provided by the bearings, it is subject to friction by rolling with possible translation sliding, which influences the real contact area between the tool/plate tribological pair. In turn, the rigid tool is only subject to sliding friction in the actual contact area at the tool/plate interface [0–0, 0].

The greater roughness on the internal surface of the cone occurred due to the friction in the contact located between the tool and the plate, and, due to the combined action of rolling and sliding friction, the roughness increased according to the freedom of rotation of the tool tip.

The F test for ANOVA (Table 5) showed that statistically the arithmetic means of the values obtained in the R_a (μm) experiments are equal, since the value obtained for the F factor was below the F-critical value.

Table 5. ANOVA for average surface roughness R_a

	F	P-value	Critical F
Rotating tool of two degrees of freedom	0.36	0.70	3.16
Rigid tool	1.89	0.16	3.16

Figure 10 shows the average of the 20 measurements for the wall thickness, with five measurements made in each quadrant of the cones. The 0 (zero) point indicates the initial thickness of the 0.8 mm part.

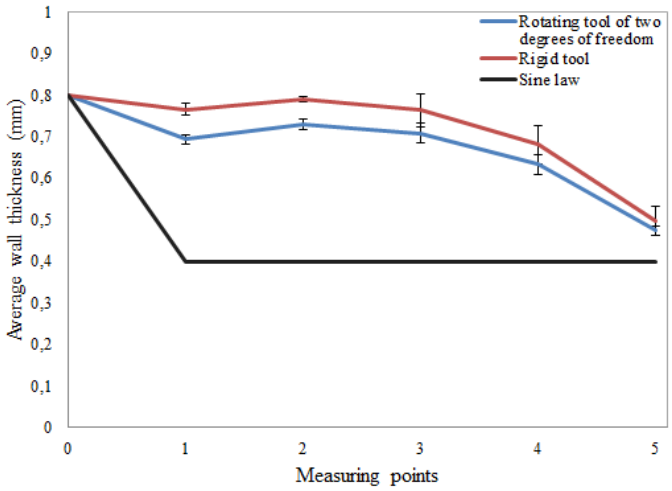

Fig. 10. Variation in thickness along the length of the straight cone

Along the cone, there is a slight variation in the thickness of the plate, according to the tool used. With the use of the rotating tool with two degrees of freedom, there was a greater reduction in thickness in relation to the rigid tool, a decrease of ~0.1mm at the beginning of the cone length. In contrast, the plates stamped with the rigid tool maintained the thickness at the beginning of the cone length at ~0.8 mm. Note that the measurements at the end of the cone (5th measurement) converged to the same thickness value for the plates stamped with both tools.

The law of sines, Eq. (2), relates the thickness to the angle of inclination of the plate, to determine its final thickness:

$$T_1 = T_0 \operatorname{sen}(90 - \varphi) \tag{2}$$

where T_1 is the minimum final thickness of the plate, T_0 is the initial thickness of the plate and φ is the angle of inclination of the wall. According to Eq. (2), with an initial thickness of 0.8 mm and a wall angle of 60º, the final thickness of the plate would be 0.41 mm. However, the final thickness obtained in the experiments was ~0.5 mm, i.e., the thickness of the plate did not follow the behaviour predicted by the law of sines; however, the experimental result obtained was close to that calculated, presenting a variation of ~23%. According to [0], the sine law is an approximate model for calculating the minimum wall thickness, as it only considers the angle of the wall, disregarding other important parameters that influence the thickness of the plate, such as the vertical increment and the tool radius.

3.4 SEM analysis

The wear mechanisms in the tools were investigated by surface morphology and variations in chemical composition, based on SEM analyses. The SEM analysis of the contact surfaces of the rotating tools with two degrees of freedom and rigid is shown in Fig. 11.

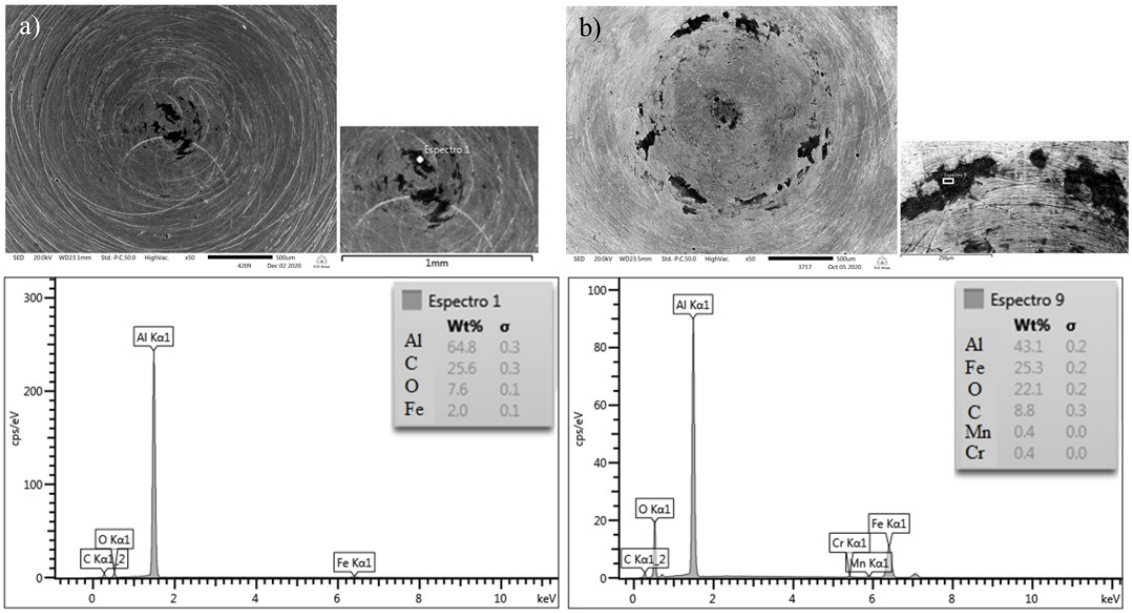

Fig. 11. MEV-EDS analysis. (a) Rigid tool. (b) Rotating tool with two degrees of freedom

From the results, it is observed that adhesion occurred at both the contact tip of the rotating tool with two degrees of freedom and the rigid tool, showing that the adhesive wear mechanism was predominant in the SPIF process, as also noted in [0, [33]-0].

Tool wear is influenced by the friction that occurs between the tool and the plate, in accordance with [0].

As the rigid tool works only with the sliding movement, the adhesion was located only in the centre of the contact tip (Fig. 11(a)).

The rotating tool with two degrees of freedom showed two well-defined regions of adhesion, one along its perimeter and the other in the centre of its tip (Fig. 11(b)). The angular adhesion located on the perimeter of this tool was caused by the rolling movement, because when the tool rolls over the surface, this is the region that is in contact. In contrast, the central adhesion was caused by the sliding movement, because

when the rotating tool slides over the surface, the central region is in contact, with adhesion occurring at that point.

Therefore, during the deformation of the aluminium sheet from the ISF process, the contact friction between the tool and the sheet, caused the removal of aluminium particles, which can slide and roll under the tool. These fragments are pressed during stamping and adhere to the surface of the tool, leading to the adhesion mechanism. As the tool advances, the adhesion points can rub against the contact surface, which generates the grooves on the surface of the plates [0, [33], 0].

The presence of the internal bearings in the tool with two degrees of freedom should, in theory, decrease this adhesive effect in comparison to the rigid tool; however, the combination of rolling friction accompanied by sliding altered the characteristics of the tribological system contributing to the elimination of the lubricating film in the contact point and favouring adhesion by chemical affinity in the rotating tool.

In addition, the characteristic of the test with the free rotation of the tools contributed to the imprisonment of aluminium particles between the tool and the plate, damaging the surface of the tool, such behaviour can be found in the work carried out in [0].

4 CONCLUSIONS

In this study, a new type of rotating tool geometry was used at the ISF. The effects of varying degrees of freedom of the contact tool on the surface roughness and wall thickness of AA1100 aluminium plates were investigated. Two types of tools (rigid and rotating with two degrees of freedom) were used to stamp the 0.8 mm-thick aluminium sheets with straight cone geometry using the SPIF method.

The choice of tool used in the incremental stamping, influenced the final quality of the desired parameters of the AA1100 aluminium sheets. The tool with two degrees of freedom improved the formability of aluminium AA1100, allowing greater depths of stamping, but did not show improvement in surface roughness, as it contributed negatively to the quality of the internal finish of the parts compared to the results obtained with the rigid tool.

Adhesive wear was predominant in the SPIF process, influencing the final roughness of the printed cones. The greater location of adhesion points on the rotating tool contributed to the increase in the final roughness of the parts stamped with this tool, due to the friction of these points with the aluminium plate.

The friction conditions (rolling or sliding) influenced the location of the aluminium adhesion on the tools. In the condition of rolling friction, the adhesion was located in the perimeter adjacent to the contact tip of the tool and in the sliding friction the adhesion was located in the centre.

ACKNOWLEDGEMENTS

The authors are grateful to CNPQ, CAPES, FAPEMIG and Pontifical Catholic University of Minas Gerais (PUC-MG) for technical support. This study was financed in part by the Coordenação de Aperfeiçoamento de Pessoal de Nível Superior - Brasil (CAPES) - Finance Code 001.

Funding: This study was financed in part by the Coordenação de Aperfeiçoamento de Pessoal de Nível Superior - Brazil (CAPES) - Finance Code 001

Conflicts of Interest: None

Availability of data and material (data transparency): Not applicable.

Code availability (software application or custom code): Not applicable.

Authors contributions: Gilmar Cordeiro da Silva: Conceptualization, Project Supervision, Experiments and Writing; Lucas Moraes Rufini de Souza: Conceptualization, Experiments, Data analysis, Writing; Lucio Flávio Santos Patrício: Data analysis, Writing.

Ethics approval (include appropriate approvals or waivers): Not applicable.

Consent to participate (include appropriate statements): Not applicable.

Consent for publication (include appropriate statements): Not applicable.

REFERENCES

[1] Ai S, Long H (2019) A review on material fracture mechanism in incremental sheet forming. Int J Adv Manuf Technol 104:33-61. https://doi.org/10.1007/s00170-019-03682-6

[2] Allwood JM, King GPF, Duflou J (2005) A structured search for applications of the incremental sheet-forming process by product segmentation. J Eng Manuf 219:239-244. https://doi.org/10.1243/095440505X8145

[3] Behera AK, Sousa RA, Ingarao G, Oleksik V (2017) Single point incremental forming: An assessment of the progress and technology trends from 2005 to 2015. J Manuf Processes 27:37-62. https://doi.org/10.1016/j.jmapro.2017.03.014

[4] Boulila A, Ayadi M, Marzouki S, Bouzidi (2018) Contribution to a biomedical component production using incremental sheet forming. Int J Adv Manuf Technol 95:2821-2833. https://doi.org/10.1007/s00170-017-1397-4

[5] Jeswiet J, Micari F, Hirt G, Bramley A, Duflou J, Allwood J (2005) Asymmetric single point incremental forming of sheet metal. CIRP annals 54:88-114. https://doi.org/10.1016/S0007-8506(07)60021-3

[6] Nasulea D, Oancea G (2017) Incremental deformation: a literature review. In MATEC Web of Conferences (Vol. 121, p. 03017). EDP Sciences. https://doi.org/10.1051/matecconf/201712103017

[7] Gatea S, Ou H, Mccartney G (2016) Review on the influence of process parameters in incremental sheet forming. Int J Adv Manuf Technol 87:479-499. https://doi.org/10.1007/s00170-016-8426-6

[8] Pathak J (2017) A brief review of incremental sheet metal forming. I International Journal of Latest Engineering and Management Research, 2(3), 35-43.

[9] Echrif SBM, Hrairi M (2011) Research and Progress in Incremental Sheet Forming Processes. Materials and Manuf Processes 26:1404-1414. https://doi.org/10.1080/10426914.2010.544817

[10] Arfa H, Bahloul R, Belhadjsalah H (2013) Finite element modelling and experimental investigation of single point incremental forming process of aluminum sheets: influence of process parameters on punch force monitoring and on mechanical and geometrical quality of parts. Int J Material Forming 6:483-510. https://doi.org/10.1007/s12289-012-1101-z

[11] Dwivedy M, Kalluri V (2019) The effect of process parameters on forming forces in single point incremental forming. Procedia Manuf 29:120-128. https://doi.org/10.1016/j.promfg.2019.02.116

[12] Lamminen L (2005) Incremental sheet forming with an industrial robot - forming limits and their effect on component design. Advanced Materials Research 6-8:457-464. https://doi.org/10.4028/www.scientific.net/AMR.6-8.457

[13] Kumar Y, Kumar S (2015) Incremental Sheet Forming (ISF). In Advances in Material Forming and Joining 29-46. Springer, New Delhi. https://doi.org/10.1007/978-81-322-2355-9_2

[14] Cristino VAM, Rosa PAR, Martins PAF (2015) The role of interfaces in the evaluation of friction by ring compression testing. Experimental Techniques 39:47-56. https://doi.org/10.1111/j.1747-1567.2012.00857.x

[15] Sornsuwit N, Sittisakuljaroen S (2014) The effect of lubricants and material properties in surface roughness and formability for single point incremental forming process. Advanced Materials Research 359-362. https://doi.org/10.4028/www.scientific.net/AMR.979.359

[16] Hussain G, Gao L (2007) A novel method to test the thinning limits of sheet metals in negative incremental forming. Int J Machine Tools and Manuf 47:419-435. https://doi.org/10.1016/j.ijmachtools.2006.06.015

[17] De Castro Maciel D, Da Silva GC, De Quadros LM (2020) Incremental stamping forming with use of roller ball tool in aluminum and magnesium alloy. Int J Adv Manuf Technol 108:455-462. https://doi.org/10.1007/s00170-020-05425-4

[18] Azhiri RB, Rahimidehgolan F, Javidpour F, Tekiyeh RM, Moussavifard SM, Bideskan AS (2020) Optimization of Single Point Incremental Forming Process Using Ball Nose Tool. Experimental Techniques 44:75-84. https://doi.org/10.1007/s40799-019-00338-8

[19] Kwan Z, Wang Z, Kang S (2008) Mechanical behavior and microstructural evolution upon annealing of the accumulative roll-bonding (ARB) processed Al alloy 1100. Materials Science and Eng 480:148-159. https://doi.org/10.1016/j.msea.2007.07.022

[20] Santos Filho O C D (2009) Caracterizações de propriedades microestruturais e mecânicas de ligas AA 1100 e AA 5052 processadas pela técnica de laminação acumulativa (Accumulated Roll Bonding-ARB). (Doctoral Dissertation) Thesis, Universidade de São Paulo.

[21] De Castro Maciel DC (2016) Comparação de duas ferramentas de contato no estudo da estampagem incremental na liga de alumínio en aw-1100. Dissertation, Pontifícia Universidade Católica de Minas Gerais

[22] Soeiro JMC (2014) Enformabilidade em estampagem incremental. Dissertation, Universidade de Lisboa

[23] Lopes TFRS (2013) Estampagem Incremental: Compensação do Retorno Elástico e Análise à Rotura. Dissertation, Universidade do Porto

[24] Ham M, Jeswiet J (2006) Single point incremental forming and the forming criteria for AA3003. CIRP annals 55:241-244. https://doi.org/10.1016/S0007-8506(07)60407-7

[25] Hirt G, Junk S, Witulski N (2002) Incremental sheet forming: quality evaluation and process simulation. *In*: Proceeding of the 7th ICTP Conference 925-930.

[26] Jawale K, Duarte JF, Reis A, Silva MB (2018) Microstructural investigation and lubrication study for single point incremental forming of copper. Int J Solids and Structures 151:145-151. https://doi.org/10.1016/j.ijsolstr.2017.09.018

[27] Castelan J (2010) Estampagem incremental do titânio comercialmente puro aplicação em implante craniano. Thesis, Universidade Federal do Rio Grande do Sul

[28] Chang Z, Chen J (2019) Analytical model and experimental validation of surface roughness for incremental sheet metal forming parts. Int J Machine Tools and Manuf 146:103453. https://doi.org/10.1016/j.ijmachtools.2019.103453

[29] Da Silva P, Alvares A (2019) Investigation of tool wear in single point incremental sheet forming. J Eng Manuf 234:170-188. https://doi.org/10.1177/0954405419844653

[30] Qu J, Xu H, Feng Z, Frederick A, Na L, Heinrich H (2011) Improving the tribological characteristics of aluminum 6061 alloy by surface compositing with sub-micro-size ceramic particles via friction stir processing. Wear 271:1940-1945. https://doi.org/10.1016/j.wear.2010.11.046

[31] Johnson K (1985) Contact mechanics. Cambridge University Press London. https://doi.org/10.1017/CBO9781139171731

[32] Cavaler LCC (2010) Parâmetros de conformação para a estampagem incremental de chapas de aço inoxidável AISI 304L. 2010. Thesis, Universidade Federal do Rio Grande do Sul

[33] Lu B, Fang Y, Xu DK, Chen J, Ou H, Moser NH, Cao J (2014) Mechanism investigation of friction-related effects in single point incremental forming using a developed oblique roller-ball tool. Int J Machine Tools and Manuf 85:14-29. https://doi.org/10.1016/j.ijmachtools.2014.04.007

[34] Diabb J, Rodríguez CA, Mamidi N, Sandoval JA, Taha-Tijerina J, Martínez-Romero O, Elías-Zúñiga A (2017) Study of lubrication and wear in single point incremental sheet forming (SPIF) process using vegetable oil nanolubricants. Wear 376:777-785. https://doi.org/10.1016/j.wear.2017.01.045

[35] Duflou J, Tunçkol Y, Szekeres A, Vanherck P (2007) Experimental study on force measurements for single point incremental forming. J Materials Processing Technology 189:65-72. https://doi.org/10.1016/j.jmatprotec.2007.01.005

[36] Petek A, Podgornik B, Kuzman K, Čekada M, Waldhauser W, Vižintin J (2008) The analysis of complex tribological system of single point incremental sheet metal forming - SPIF. Strojniški vestnik 54:266-273. http://www.dlib.si/details/URN:NBN:SI:doc-7BJ4ZQL9

[37] Kumar V, Kumar R (2020) Investigation of Surface Roughness in Incremental Sheet Forming of AA 2014-T6 using Taguchi's Method. *In*: J Physics: Conference Series. IOP Publishing. https://doi.org/10.1088/1742-6596/1519/1/012009